PHYSICAL REVIEW B **80**, 220501(R) (2009)

# Dynamic response and ordering of rotating vortices in superconducting Corbino disks

S. Okuma and Y. Yamazaki
*Research Center for Low Temperature Physics, Tokyo Institute of Technology, 2-12-1 Ohokayama, Meguro-ku, Tokyo 152-8551, Japan*

N. Kokubo
*Center for Research and Advancement in Higher Education, Kyushu University, 744 Moto-oka, Nishi-ku, Fukuoka 819-0395, Japan*
(Received 18 August 2009; published 2 December 2009)

We study the dynamic response of weakly disordered vortex lattice driven by a radial current $I$ in amorphous superconducting films with a Corbino geometry, where vortices rotate around the center of the sample by a frustrated Lorentz force inversely proportional to the radius. With increasing $I$, the vortices near the center are first depinned, indicative of the plastic-flow-like rotation, which gradually approaches a laminarlike flow at large $I$. We observe a mode-locking resonance, which suggests the formation of rotating vortex rings composed of triangular-lattice arrays. The field evolution of the resonance shows the presence of the lattice rotation of the driven vortex rings with respect to the flow direction.

DOI: 10.1103/PhysRevB.80.220501 PACS number(s): 74.40.+k, 62.20.F−, 74.25.Qt, 74.78.Db

Magnetic-flux lines (vortices) penetrating type-II superconductors form a solid or liquid phase depending on the strength of magnetic field $B$ or temperature $T$. It is of practical importance to study how the vortices respond dynamically to an applied current because the vortex motion gives rise to dissipation. Fundamentally, studies of moving vortex matter provide useful information for understanding physics of self-assembled objects subjected to shearing forces and their collective behaviors. A prominent example is the vortex dynamics confined in a Corbino disk (CD),[1–6] where a radial current $I$ drives the vortices in concentric circles without crossing the sample edges by a frustrated Lorentz force inversely proportional to the radius $r$ of rotation. To date, interesting dynamic transitions of vortex matter have been reported in CD as a function of $I$, which include the elastic to plastic flow transition, as observed in YBCO,[3] and a tearing transition of the elastic disk, as predicted by simulation.[2,6] These studies lead to new insights into friction at a solid-solid interface and plastic motion of solids,[1,2] which are widely observed in nature but hardly understood, in particular, at a microscopic scale.

We have recently studied transverse velocity correlations of rotating vortices in amorphous ($a$-)$Mo_xGe_{1-x}$ films as a function of $B$ by measuring the current-voltage ($I-V$) characteristics at the two voltage probes placed radially.[7] As $I$ is increased in the solid phase (weakly disordered lattice), the vortices near the center are first depinned, indicative of the plastic-flow-like rotation instead of the elastic rotation. With further increasing $I$, the plastic flow gradually transforms into laminar(liquid)like flow. Although the elastic rotation is absent due probably to larger pinning strength and/or larger sample sizes, some elasticity may survive in the plastic or laminarlike flow states. To explore this issue, we conduct here measurements of a mode-locking (ML) resonance. Using this technique, we are able to detect the periodicity of the rotating vortices in the circumferential direction.

We study $a$-$Mo_xGe_{1-x}$ films with electrical contacts, which enable us to measure vortex dynamics comparatively in CD and striplike (SL) configurations on the same sample. Using the ordinary rectangular films of $a$-$Mo_xGe_{1-x}$, detailed data of ML have been obtained.[8–10] We observe the ML resonance for both CD and striplike geometries and find that moving vortex matter in CD is vortex rings composed of triangular vortex arrays with different $r$. In high fields $B$, the orientation of the triangular array with respect to the flow direction (i.e., circumferential direction) is perpendicular to the one side of the triangle(s). With decreasing $B$, the orientation changes from perpendicular to parallel.

Two 330-nm-thick $a$-$Mo_xGe_{1-x}$ films (films 1 and 2) were prepared by rf sputtering on Si substrates held at room temperature.[8–10] The mean-field transition temperature defined by a 95% criterion, i.e., the temperature at which the resistivity decreases to 95% of the normal-state resistivity, and the zero-resistivity temperature for both films are 6.3 and 6.2 K, respectively. At 4.1 K, where all the data were taken, the upper-critical field $B_{c2}$ defined by the 95% criterion[11] is 4.8–4.9 T. The Ohmic resistivity vanishes at 3.8–3.9 T($\equiv B_c$), which separates the vortex solid in lower fields ($<B_c$) from the vortex liquid in higher fields ($>B_c$). The arrangement of silver electrical contacts is shown schematically in the inset of Fig. 1. The similar contact arrangement was used originally by Paltiel *et al.*[12] For the measurements in the CD geometry, the current flows between the contact +C of the center and that −C of the perimeter of the disk, which produces radial current density that decays as $1/r$. For the striplike geometry, contacts $+S$ and $-S$ were used. In the striplike configuration, the current-flow pattern is nonuniform except around the center of the sample; i.e., it has a component normal to the line connecting points $+S$ and $-S$, similar to the situation with a Hall-cross geometry,[13] and the vortex motion is not completely straight near the sample edges.[14] For both geometries, we used the same voltage contacts $P_1$, $P_2$, and $P_3$ (indicated with 1, 2, and 3 in the inset). The inner radius of CD is 2.3 and 0.8 mm for films 1 and 2, respectively. For film 1, the distances from the center of the sample to (the center of) the contacts $P_1$, $P_2$, and $P_3$ are, respectively, $CP_1=0.85$, $CP_2=1.45$, and $CP_3=1.90$ mm, which serve as the two voltage probes ($V_{12}$ and $V_{23}$) with different radii $r_{12}$ and $r_{23}$ ($r_{12}<r_{23}$). For film 2, $CP_1=0.25$ and $CP_2=0.37$ mm. The field $B$ was applied perpendicular to the plane of the film. In the measurements of ML for film 2, we superimposed ac current $I_{ac}$ with frequency

 

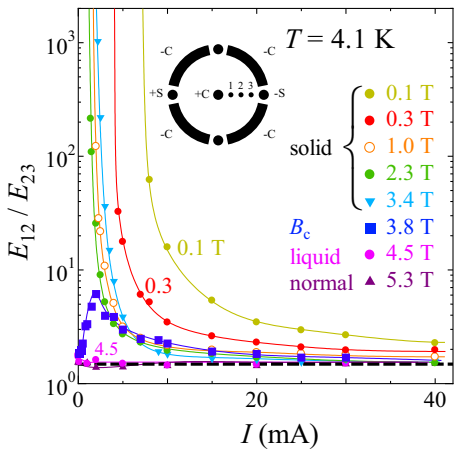


FIG. 1. (Color online) $E_{12}/E_{23}$ vs $I$ of film 1 at 4.1 K in different $B$:0.1–3.4 (solid phase), 3.8($B_c$), 4.5 (liquid phase), and 5.3 T (normal phase). In 1.0 T, for example, $I_c$ at $r_{12}$ is 0.75 mA, where $E_{12}/E_{23} \to \infty$. A dashed line indicates the liquidlike rotation. Other lines are guides for the eyes. Inset: the arrangement of the electrical contacts.

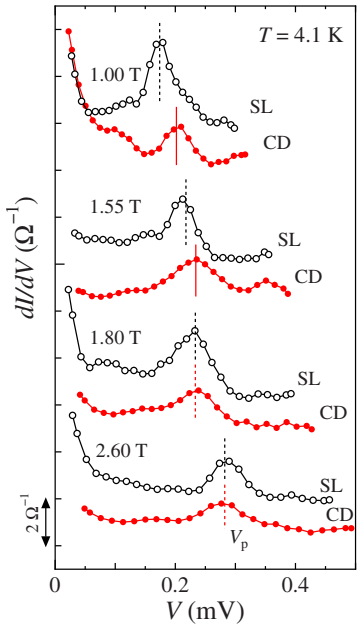


FIG. 2. (Color online) $dI/dV$ vs $V$ of film 2 at 4.1 K in different $B$ in the presence of superimposed (35 MHz) $I_{ac}$ for CD (full circles) and striplike (SL) (open circles) geometries. Location of $V_{1/2}^{perp}$ and $V_{1/1}^{para}$ calculated assuming the perpendicular and parallel lattice orientation is indicated with vertical dashed and full lines, respectively. Other lines are guides for the eyes. The curves are vertically shifted for clarity.

$f_{ext}$=35 MHz on dc current $I$. The films were directly immersed in liquid $^4$He to ensure good thermal contact.

We summarize the results of dc $I-V$ characteristics for film 1 measured at $r_{12}$ and $r_{23}$ in the CD geometry. In the vortex liquid, the $I-V$ curve is linear over the current range measured, irrespective of $r$. The voltage in the inner part ($r_{12}$) is larger by a geometrical factor of ~1.5 than that for outer part ($r_{23}$) due to the $r$-dependent driving current. Meanwhile, in the vortex solid ($B<3.8$ T), the $I-V$ curves show strong nonlinearity and the voltage responses are highly $r$ dependent. The voltage in the inner part is much larger than that in the outer part. This difference is significant near the depinning current $I \sim I_c$, where a detectable voltage appears only in the inner part and it is absent in the outer part. These characteristics are well displayed by plotting the ratio of $E_{12}/E_{23}$, where $E_{12}$ and $E_{23}$ are the average electric fields at $r_{12}$ and $r_{23}$, respectively. In the main panel of Fig. 1, we plot the $I$ dependence of $E_{12}/E_{23}$ at constant $B$ ranging from 0.1 T (vortex solid) to 5.3 T (normal phase). In 4.5 T (vortex liquid), the data points of $E_{12}/E_{23}$ fall onto nearly an $I$-independent (dashed) line, which is consistent with the behavior expected for the liquid(laminar)like rotation. By contrast, in lower $B$=0.1–3.4 T, $E_{12}/E_{23}$ takes significant large values at low $I$ due to the large velocity gradient developed in the radial direction, indicative of the pinning-dominated plastic-flow-like rotation. As $I$ is increased, $E_{12}/E_{23}$ decreases monotonically and approaches the dashed line for the liquidlike rotation at large $I$, suggesting the current-induced gradual transformation from the plastic flow to the laminar flow at large enough $I$.

We perform the ML measurements of driven solid in the flow state close to the laminar flow for film 2. Now, we briefly explain the ML technique. When an elastic medium moves in a periodic potential in the presence of combined dc and ac forces, steplike structure analogous to Shapiro steps found in Josephson junctions appears in $I-V$ characteristics.[15–19] The steps appear when an internal frequency of the system locks to an external frequency $f_{ext}$ of the ac drive. This phenomenon called the ML resonance has been observed not only in superconductors with periodic pinning[17,18] but also in those with random pinning,[15,19] such as amorphous films studied here, where a periodicity can be induced dynamically as a result of the coherent motion[20,21] of a vortex lattice.

In our previous measurements for rectangular $a$-$Mo_xGe_{1-x}$ films, we obtained clear evidence for ML resonance.[8–10] In the intermediate fields between 1 and 3.5 T at 4 K, which correspond to the ordered phase with a weakly disordered vortex lattice,[22] driven vortices form a triangular vortex array moving in the direction perpendicular to one side of the triangle(s), which we call the perpendicular orientation. The lattice period $a_\perp$ in the direction of vortex motion is equal to $(2\sqrt{3}\Phi_0/B)^{1/2}$, where $\Phi_0$ is the flux quantum. The observed first ML step voltage ($V_{p/q}^{perp}$) satisfies the subharmonic resonant condition of $p/q=1/2$; i.e., $V_{1/2}^{perp}[=l(p/q)f_{ext}a_\perp B] = lf_{ext}(\sqrt{3}\Phi_0 B/2)^{1/2}$, where $l$ is the distance between the voltage contacts.

For the *striplike* geometry studied in this work, we observe ML peaks in the $dI/dV$ vs $V$ curves. Selected data in $B$=1.00, 1.55, 1.80, and 2.60 T are shown with open circles in Fig. 2.[14] For each field, the first ML voltage $V_{peak}^{SL}$ again corresponds to the subharmonic $V_{1/2}^{perp}$,[10] as indicated with a vertical dashed line. We see good agreement between measured $V_{peak}^{SL}$ and calculated $V_{1/2}^{perp}$ for all the fields studied (see the following discussion on Fig. 3) as well as for the selected fields in Fig. 2.

For the CD geometry, we also observe ML peaks in the

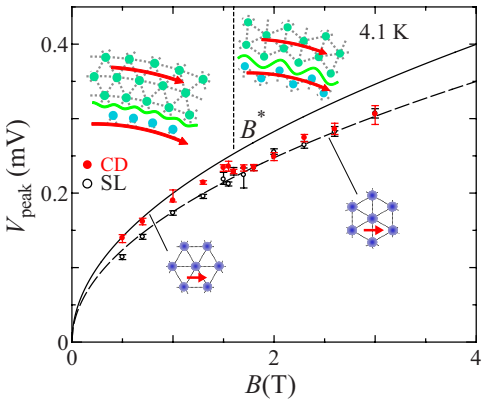


FIG. 3. (Color online) $B$ dependences of $V_{peak}^{CD}$ (full circles) and $V_{peak}^{SL}$ (open circles) of film 2 at 4.1 K for CD and striplike geometries, respectively. Dashed and full lines, respectively, represent $V_{1/2}^{perp}$ and $V_{1/1}^{para}$. Insets: schematic diagrams for triangular vortex arrays, where arrows indicate the direction of the vortex motion.

$dI/dV$ vs $V$ curves for all $B$ studied. However, the peak shape looks broader than that for the striplike geometry and higher-order peaks are invisible. They are attributed to the velocity gradient developed between the voltage contacts ($P_1P_2 \approx 0.1$ mm). Using $CP_1=0.25$ and $CP_2=0.37$ mm and assuming the vortex-velocity profile in the form $v(r) \propto 1/r$ for (close to) the laminar flow state, the distribution of $v(r)$ and $V_{peak}^{CD}(r)$ along the interval $P_1P_2$ is estimated to be about $\pm 20\%$ around their mean values. The selected data of $dI/dV$ vs $V$ taken in 1.00, 1.55, 1.80, and 2.60 T are shown with full circles in Fig. 2, which are compared with those (open circles) for the striplike geometry. In 1.80 and 2.60 T, the peak voltage $V_{peak}^{CD}(B)$ for the CD geometry is identical to that $V_{peak}^{SL}(B)$ for the striplike geometry (dashed lines). The results indicate that the elasticity survives in the rotating vortices and that the flow state studied in this work is not a complete laminar or liquid-flow state in which the transverse vortex-velocity correlation is absent down to a microscopic scale. The present results strongly suggest the formation of rotating vortex rings that are composed of triangular vortex arrays with the perpendicular orientation. Since the ML technique enables us to detect only the periodicity of the rotating vortices in the circumferential direction, it does not evidence, in principle, the transverse periodicity of the vortex rings. Some smecticlike vortex arrangement, as revealed by scanning tunneling spectroscopy on the static vortex states,[23] may be also realized in our rotating vortex rings in the mode-unlocked state. However, the ML resonance makes the vortex system more ordered and each vortex ring is well described by the triangular lattice.

In lower fields (1.0 and 1.55 T), $V_{peak}^{CD}(B)$ for the CD geometry takes the values approximately 15% larger than those for the striplike geometry; i.e., $V_{peak}^{CD}(B) \approx 1.15 V_{peak}^{SL}(B)$. The resonant voltage of the first ML peak $V_{peak}^{CD}$ is consistent with the condition for the parallel lattice orientation given by $V_{1/1}^{para}=(2/\sqrt{3})V_{1/2}^{perp}$, as indicated with vertical full lines in Fig. 2. Thus, in the lower fields triangular vortex arrays in the rotating vortex rings have *parallel* orientation with respect to the flow direction.

In order to see how the lattice orientation changes with $B$, we show in Fig. 3 the field dependences of $V_{peak}^{CD}$ (full circles) for the CD geometry together with $V_{peak}^{SL}$ (open circles) for the striplike geometry. For the CD geometry, $V_{peak}^{CD}(B)$ in high fields $B=1.8-3.0$ T follows the resonant condition for the perpendicular orientation displayed by a dashed curve, whereas in lower fields $B=0.5-1.5$ T it agrees with the parallel resonant condition (indicated with a full curve) given by $V_{1/1}^{para}(B)=(2/\sqrt{3})V_{1/2}^{perp}(B)$. Thus, the lattice orientation of rotating vortex rings changes at $\sim 1.6 \pm 0.2$ T($\equiv B^*$).

There is no available theory to account for the remarkable findings and we consider here the qualitative interpretation of the data. In general, the dynamics of driven vortex matter is described by a driving force due to an applied current, the vortex-vortex interaction, as determined by an applied field, and the random pinning potential due to quenched disorder. For the CD geometry studied in this work, the perpendicular lattice orientation similar to that found in the rectangular films is observed above the crossover field $B^*$, as schematically illustrated in the inset (top right) of Fig. 3. Here, arrows and a wavy line, respectively, indicate the velocity of the rotating rings and the interface between adjacent rings that slip with respect to each other. When the shearing force ($\propto 1/r$), acting on the rotating vortices, in the presence of random pinning, dominate over the "friction" force at the interface, the slip between the adjacent rings will take place, as observed in our films. In case of the perpendicular lattice orientation, the largest shearing force is needed to induce the slip of the rings.

As the field is lowered below $B^*$ and the vortex-vortex interaction becomes small, the configuration of the rings may change from the perpendicular to parallel orientation. This is schematically illustrated in the inset (top left) of Fig. 3, where the interface between adjacent rings is smoother than for the perpendicular orientation. This leads to the suppression of the energy barrier that the adjacent rings must overcome in order to slip against each other and to the release of the frustration (shear stress concentration) accumulated in the vortex system. Within this interpretation, the observed change in the lattice orientation with decreasing field may be associated with the decrease in the elasticity of the vortex lattice in the presence of shear and pinning forces.

The results obtained in our work indeed await theoretical explanations, e.g., the exact meaning of $B^*$ is still unclear. Naively, the experimental value of $B^* \approx 0.3 B_{c2}$ does not look small enough to make the vortex lattice softer. Meanwhile, it has been shown numerically[24] that in mesoscopic CD subtle changes in vortex-ring configuration, i.e., (in)commensurability effects between adjacent vortex shells, play a crucial role in vortex dynamics, giving rise to unconventional vortex motion. It is interesting to study numerically how the behavior changes in larger CD, as studied in our work. The phenomena observed in this work are novel and we believe that they will stimulate further theoretical and experimental investigations. Also, this work shows clearly that the ML technique, combined with $I-V$ measurements, is a useful probe to explore plasticity and tearing phenomena of solids subjected to shearing forces from the microscopic viewpoint.

This work was supported by a Grant-in-Aid for Scientific Research from the Ministry of Education, Culture, Sports, Science, and Technology of Japan.

[1] G. W. Crabtree, Nature Mater. **2**, 435 (2003).
[2] M.-C. Miguel and S. Zapperi, Nature Mater. **2**, 477 (2003).
[3] D. López, W. K. Kwok, H. Safar, R. J. Olsson, A. M. Petrean, L. Paulius, and G. W. Crabtree, Phys. Rev. Lett. **82**, 1277 (1999).
[4] V. R. Misko and F. M. Peeters, Phys. Rev. B **74**, 174507 (2006).
[5] S. F. W. R. Rycroft, R. A. Doyle, D. T. Fuchs, E. Zeldov, R. J. Drost, P. H. Kes, T. Tamegai, S. Ooi, and D. T. Foord, Phys. Rev. B **60**, R757 (1999).
[6] A. Furukawa and Y. Nisikawa, Phys. Rev. B **73**, 064511 (2006).
[7] S. Okuma, Y. Suzuki, Y. Yamazaki, and N. Kokubo, Physica C **468**, 1322 (2008), and references therein.
[8] N. Kokubo, T. Asada, K. Kadowaki, K. Takita, T. G. Sorop, and P. H. Kes, Phys. Rev. B **75**, 184512 (2007).
[9] S. Okuma, J. Inoue, and N. Kokubo, Phys. Rev. B **76**, 172503 (2007).
[10] N. Kokubo, B. Shinozaki, and P. H. Kes, Physica C **468**, 581 (2008).
[11] S. Okuma, Y. Imamoto, and M. Morita, Phys. Rev. Lett. **86**, 3136 (2001).
[12] Y. Paltiel, E. Zeldov, Y. Myasoedov, M. L. Rappaport, G. Jung, S. Bhattacharya, M. J. Higgins, Z. L. Xiao, E. Y. Andrei, P. L. Gammel, and D. J. Bishop, Phys. Rev. Lett. **85**, 3712 (2000).
[13] A. V. Silhanek, J. Van de Vondel, V. V. Moshchalkov, A. Leo, V. Metlushko, B. IIic, V. R. Misko, and F. M. Peeters, Appl. Phys. Lett. **92**, 176101 (2008).
[14] This will explain the fact that compared to the case of the rectangular films (Refs. 8 and 9), the ML signal in the striplike geometry looks somewhat degraded, as shown in Fig. 2.
[15] A. T. Fiory, Phys. Rev. Lett. **27**, 501 (1971).
[16] M. J. Higgins, A. A. Middleton, and S. Bhattacharya, Phys. Rev. Lett. **70**, 3784 (1993).
[17] L. Van Look, E. Rosseel, M. J. Van Bael, K. Temst, V. V. Moshchalkov, and Y. Bruynseraede, Phys. Rev. B **60**, R6998 (1999).
[18] C. Reichhardt, R. T. Scalettar, G. T. Zimányi, and N. Grønbech-Jensen, Phys. Rev. B **61**, R11914 (2000).
[19] N. Kokubo, K. Kadowaki, and K. Takita, Phys. Rev. Lett. **95**, 177005 (2005).
[20] Y. Togawa, R. Abiru, K. Iwaya, H. Kitano, and A. Maeda, Phys. Rev. Lett. **85**, 3716 (2000).
[21] A. E. Koshelev and V. M. Vinokur, Phys. Rev. Lett. **73**, 3580 (1994).
[22] S. Okuma, K. Kashiro, Y. Suzuki, and N. Kokubo, Phys. Rev. B **77**, 212505 (2008).
[23] I. Guillamón, H. Suderow, A. Fernández-Pacheco, J. Sesé, R. Córdoba, J. M. De Teresa, M. R. Ibarra, and S. Vieira, Nat. Phys. **5**, 651 (2009).
[24] N. S. Lin, V. R. Misko, and F. M. Peeters, Phys. Rev. Lett. **102**, 197003 (2009).